

We SBT5 02

## Hydromechanical Simulation of Hydraulic Fracturing in Naturally Fractured Reservoir Using Strong Discontinuity Approach

L.B. Beserra\* (Federal University of Pernambuco), L.N. Guimaraes (Federal University of Pernambuco) & O.L. Manzoli (State University of São Paulo)

### SUMMARY

---

Hydraulic Fracturing is a widely used method for enhancing oil exploitation in petroleum industry. In this method, some artificial fractures are induced in the reservoir by fluid injection and the overall rock permeability is increased. The geometry of the induced fracture is dominated by the rock's mechanical properties, in-situ stresses, and local heterogeneities such as natural fractures and weak bedding planes. In this paper, a strong discontinuity approach, to embed discontinuities into finite elements was implemented in a numerical code, which performs numerical analysis of fluid flow in a deformable reservoir. This technique is based on the decomposition of the displacement field, inside the element, into a component associated with the deformation of the continuum portion and a component related to the rigid-body relative motion between the two parts of the element. Moreover, the traction continuity condition must be imposed to ensure a correct relationship between the tractions on the internal interface and the stresses in the surrounding continuum portion. Hydromechanical coupling was determined by a law that relates the variation of transmissivity as a function of the fracture aperture. The resulting numerical code was used to model hydraulic fracture propagation through naturally fractured reservoirs in a very efficient manner.

## Introduction

Hydraulic Fracturing is a widely used method for enhancing oil exploitation in petroleum industry. In this method, some artificial fractures are induced in the reservoir by fluid injection and the overall rock permeability is increased. The geometry of the induced fracture is dominated by the rock's mechanical properties, in-situ stresses, and local heterogeneities such as natural fractures and weak bedding planes.

Hydraulic fractures usually propagate perpendicular to the direction of least principal stress, because this is the direction that defines the lowest work (Hubbert and David, 1972). However, modeling hydraulic fracturing in the presence of a natural fracture network is a challenging task, due to the strong coupling that exists between fluid flow and mechanical behavior, as well as the complex interactions between propagating fractures and existing natural interfaces (Hagström and Adams, 2012; Zhang *et al.*, 2010). Understanding these complex interactions through numerical modeling is critical to the optimum design of stimulation strategies.

From the mathematical point of view it is a coupled hydro-mechanical problem, where equations for fluid flow through porous media and fractures (fluid mass balance) and medium deformation and fracture propagation (mechanical problem) have to be solved simultaneously considering the constitutive equations that describe the material behavior. When a fracture propagates through a continuous media, discontinuities in the displacement and fluid pressure fields are introduced. The selection of an appropriate fracture propagation model is a critical task in modeling of hydraulic fracturing.

## Strong Discontinuity Approach

In this paper, a strong discontinuity approach, proposed by Manzoli and Shing (2006), to embed discontinuities into finite elements was implemented in the numerical code CODE\_BRIGHT (Guimarães *et al.*, 2007; Olivella *et al.*, 1994), which performs numerical analysis of fluid flow in a deformable reservoir.

To properly derive embedded discontinuity finite element formulations, fundamental aspects regarding to the kinematics and statics of the discontinuity must be considered. The kinematic enrichment must correctly reflect the position of the interface in the element as well as the relative displacement (opening and sliding) between the two opposite faces of the interface. Furthermore, the traction continuity condition must be properly imposed to ensure a correct relationship between the tractions in the internal interface and the stresses in the surrounding continuum portion.

Consider the triangular element with three nodes from domain  $\Omega_e$ , length  $l_e$ , with a band of strain localization  $S_e$ , width  $k$ , which divides the element into two parts, isolating the node 1 from nodes 2 and 3, as shown in Fig 1.

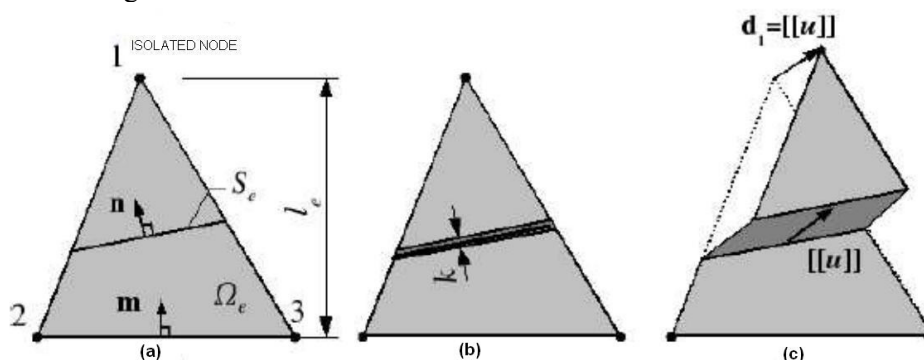


**Figure 1** Finite Element crossed by a localization band (Manzoli and Shing, 2006.).

The displacement field jump,  $[[\mathbf{u}]]$ , on  $S$  lead to a rigid-body relative motion, as shown in Fig1(c), driving to the following nodal displacements,

$$d_i = [[\mathbf{u}]]; d_2 = \mathbf{0}; d_3 = \mathbf{0} \quad (1)$$

where  $(i = 1, 2, 3)$  represents the vector of nodal displacements of node  $i$ , due to the jump in the displacement field  $[[\mathbf{u}]]$ .

The deformation of the continuum portion can be obtained from the standard finite element strain-displacement relationship,

$$\boldsymbol{\varepsilon} = \sum_{i=1}^3 \mathbf{B}_i (\mathbf{D}_i - \mathbf{d}_i) = \sum_{i=1}^3 \mathbf{B}_i \mathbf{D}_i - \mathbf{B}_1 [[\mathbf{u}]] = \mathbf{B}\mathbf{D} - \boldsymbol{\varepsilon}^R \quad (2)$$

where  $\mathbf{D}_i$  is the nodal displacement vector and  $\mathbf{B}_i$  is the standard finite element strain-displacement matrix. Considering the vectors  $\mathbf{n}$ , normal to the discontinuity, and  $\mathbf{m}$ , normal to the opposite side of the isolated node, as shown in Fig1(a). The deformation due to the displacement field jump can be written as:

$$\begin{Bmatrix} \varepsilon_x^R \\ \varepsilon_y^R \\ \gamma_{xy}^R \end{Bmatrix} = \frac{1}{l_e} \begin{bmatrix} m_x & 0 \\ 0 & m_y \\ m_y & m_x \end{bmatrix} \begin{Bmatrix} [[\mathbf{u}]]_x \\ [[\mathbf{u}]]_y \end{Bmatrix} = \frac{\mathbf{M}}{l_e} [[\mathbf{u}]] \quad (3)$$

where  $\mathbf{M}$  is a matrix containing the value of  $\mathbf{m}$  vector components and  $l_e$  is the distance between the isolated node and the opposite side of the element, as shown in Figure 2(a).

The corresponding stress field is given by:

$$\boldsymbol{\sigma} = \boldsymbol{\Sigma}^C (\boldsymbol{\varepsilon}) = \boldsymbol{\Sigma}^C \left( \mathbf{B}\mathbf{D} - \frac{\mathbf{M}}{l_e} [[\mathbf{u}]] \right) \quad (4)$$

where  $\boldsymbol{\Sigma}^C$  is the material constitutive matrix of the continuum portion, for simplicity, the continuum is considered linearly elastic and isotropic. Therefore, the vector of internal forces corresponding to the finite element with area  $A_e$ , is given by:

$$\mathbf{f}_{\text{int}} = \int_{\Omega_e} \mathbf{B}^T \boldsymbol{\sigma} d\Omega_e = \mathbf{B}^T \boldsymbol{\sigma} A_e = \mathbf{B}^T \boldsymbol{\Sigma}^C \left( \mathbf{B}\mathbf{D} - \frac{\mathbf{M}}{l_e} [[\mathbf{u}]] \right) A_e \quad (5)$$

The deformation and its corresponding stress in the localization band can be written as follows:

$$\boldsymbol{\varepsilon}_S = \boldsymbol{\varepsilon} + \frac{\mathbf{N}}{k} [[\mathbf{u}]] = \mathbf{B}\mathbf{D} - \frac{\mathbf{M}}{l_e} [[\mathbf{u}]] + \frac{\mathbf{N}}{k} [[\mathbf{u}]] \quad (6)$$

$$\boldsymbol{\sigma}_S = \boldsymbol{\Sigma}^S (\boldsymbol{\varepsilon}_S) \quad (7)$$

where  $k$ , denotes the bandwidth of strain localization,  $\boldsymbol{\Sigma}^S$  is the constitutive matrix of the discontinuity surface and.  $\mathbf{N}$  is a matrix obtained from the components of the normal vector  $\mathbf{n}$ , as:

$$\mathbf{N} = \begin{bmatrix} n_x & | & 0 \\ 0 & | & n_y \\ n_y & | & n_x \end{bmatrix} \quad (8)$$

The surface forces in the region of localization band must be in equilibrium with the forces calculated in the surround (point in the continuous portion which borders the band):

$$\mathbf{N}^T (\boldsymbol{\sigma}_S - \boldsymbol{\sigma}) = \mathbf{0} \quad (8)$$

replacing the Eq. (4) e (7) in (9):

$$\mathbf{N}^T \boldsymbol{\Sigma}^S \left( \mathbf{B}\mathbf{D} - \frac{\mathbf{M}}{l_e} [[\mathbf{u}]] + \frac{\mathbf{N}}{k} [[\mathbf{u}]] \right) - \mathbf{N}^T \boldsymbol{\Sigma}^C \left( \mathbf{B}\mathbf{D} - \frac{\mathbf{M}}{l_e} [[\mathbf{u}]] \right) = 0 \quad (9)$$

The displacement jump,  $[[\mathbf{u}]]$ , can be obtained solving the Eq (10), for a given state of strain, through the iterative method of Newton-Raphson. Since the jump components are determined, the stress tensor in the element can be obtained by Eq (4).

### Variation law of permeability

The hydro-mechanical coupling has been determined by a law that relates the variation of permeability as a function of the displacement jump from the mechanical problem, as follow:

$$k_S = \frac{[[\mathbf{u}]]_n^2}{12} \quad (11)$$

where  $[[\mathbf{u}]]_n$  is the normal jump aperture.

### Examples

The presence of natural fractures includes an additional difficulty for the modeling of hydraulic fracturing, since they may affect the fluid flow in the reservoir and the orientation of the induced fracture. In order to apply the formulation presented in this paper, the hydraulic fracturing problem in reservoirs with pre-existing fractures was simulated. A numerical tool was used to embed the natural fracture network into the finite element mesh (as illustrated in Fig 2), with respect to the geological mapping of these fractures. To model the mechanical behaviour of material, was adopted a tensile damage model proposed by Sánchez *et al.* (2014).

To evaluate the effect of initial stress state in the direction of the induced fractures , the simulations were performed considering two different scenarios for the initial stress state. Some results of the simulation are presented in Fig 3.

When the initial stress state is isotropic , there is no preferential direction for the opening of the fracture and propagation occurs following the way of the first natural fractures that are pressurized, meanwhile, for the anisotropic stress state a main fracture is open in the direction of the maximum principal stress and natural fractures that connect with the main one are also pressurized promoting the increase of the permeability surrounding the main fracture.

Also, in both scenarios , when the stress state in the tip of the fracture overcomes the tensile strength of the rock, occurs propagation of the fracture through the intact rock , this effect contributes to the formation of a network interconnecting fractures previously not conected.

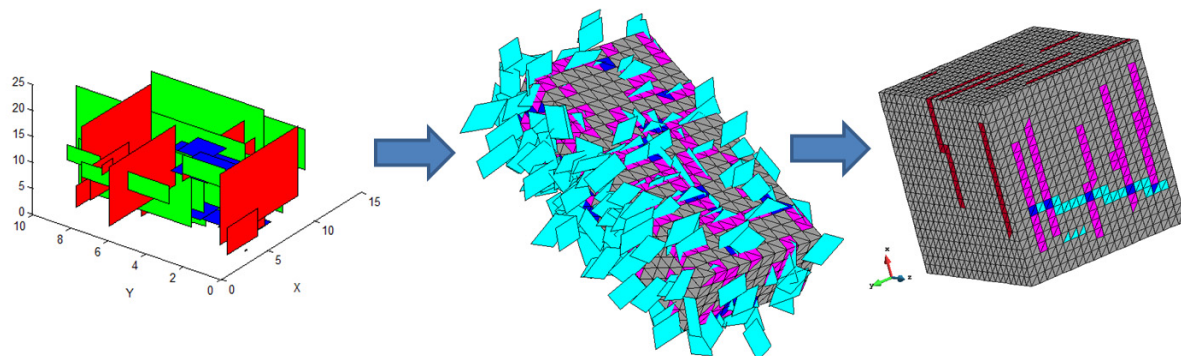


**Figure 2** The stages to embed natural fractures network in Finite Element Meshes.

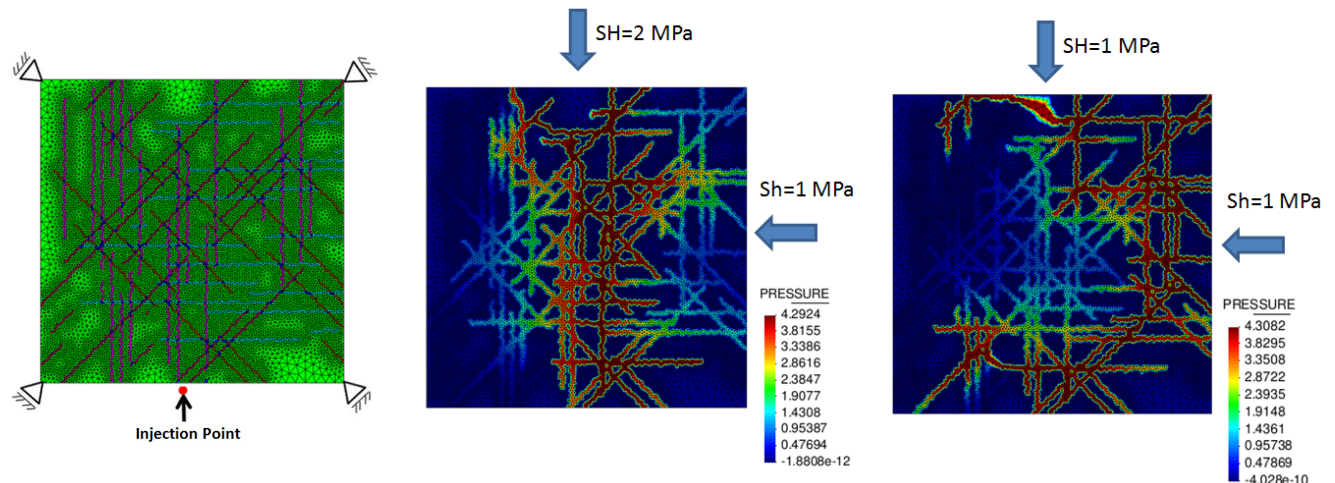


**Figure 3** Effect of initial stress state on the final pattern of hydraulic induced and reactivated fractures.

## Conclusions

The resulting numerical code was used to model hydraulic fracture propagation through naturally fractured reservoirs with relatively coarse meshes in a reasonable computational time. Furthermore, the results provided an important insight into the mechanisms that generate microseismicity that occurs during hydraulic fracture stimulation. The interpretation of microseismicity based on geomechanical analysis gives a more realistic estimation of the stimulated reservoir volume (SRV), otherwise SRV can be overestimated.

## Acknowledgements

This research was supported by CNPq/Brazil, Petrobras and Foundation CMG. The third author wishes to acknowledge the financial support of the Sao Paulo Research Foundation (FAPESP, grant #2013/01742-0).

## References

- Guimarães, L.N., Gens, A., Olivella, S. [2007] Coupled thermo-hydro-mechanical and chemical analysis of expansive clay subjected to heating and hydration. *Transport in Porous Media*, **66**, 341–372.
- Hagström, E.L. and Adams, J.M. [2012] Hydraulic Fracturing: Identifying and Managing the Risks. *Environmental Claims Journal*, **24**, 93-115.
- Hubbert, M.K. and David, G.W. [1972] Mechanics of hydraulic fracturing. *Transactions of Society of Petroleum Engineers of AIME*, **210**, 153-168.
- Manzoli, O.L. and Shing, P.B. [2006] A general technique to embed non-uniform discontinuities into standard solid finite elements. *Computers & Structures*, **84**, 742–757.
- Olivella, S., Carrera, J., Alonso, E. [1994]. Nonisothermal multiphase flow of brine and gas through saline media. *Transport in Porous Media*, **15**, 271–293.
- Sánchez, M.; Manzoli, O. L.; Guimarães, L. J. N. [2014] Modeling 3-D desiccation soil crack networks using a mesh fragmentation technique. *Computers and Geotechnics*, **62**, 27-39.
- Zhang, G.M., Liua, H., Zhang, J., Wua, H.A., Wang, X.X. [2010] Three-dimensional finite element simulation and parametric study for horizontal well hydraulic fracture. *Journal of Petroleum Science and Engineering*, **72**, 310-317.